

# Improved stability regions for ground states of the extended Hubbard model

Zsolt Szabó<sup>a</sup>

*Institut für Theoretische Physik, Universität zu Köln, Zùlpicher Str. 77, D-50937 Köln, Germany*  
(31 December 1998)

The ground state phase diagram of the extended Hubbard model containing nearest and next-to-nearest neighbor interactions is investigated in the thermodynamic limit using an exact method. It is found that taking into account local correlations and adding next-to-nearest neighbor interactions both have significant effects on the position of the phase boundaries. Improved stability domains for the  $\eta$ -pairing state and for the fully saturated ferromagnetic state at half filling have been constructed. The results show that these states are the ground states for model Hamiltonians with realistic values of the interaction parameters.

PACS number: 74.20.-z, 75.10.Jm, 75.10.Lp

## I. INTRODUCTION

Exact solutions in physics are of great importance, since in some cases the errors introduced by the approximations may dominate the results to such an extent that one might end up with an incorrect description of the studied phenomenon. When applying an analytic, but non-exact, approach one has to know to what extent the approximation is valid. In case of perturbative methods a well-defined *small* parameter can ensure that the higher order terms are indeed negligible. Often, it is hard to find such a small parameter due to the fact that the given phenomenon itself has strong-coupling characteristics, i.e. the associated correlation effects are not small at all. This is especially true by the investigation of strongly correlated electron systems. Ferromagnetism is an example for *intermediate-to-strong* coupling phenomenon, where one has to be very cautious to apply perturbative approaches.

Considering the exact results with respect to the dimensionality  $D$ , we can see that most of them have been derived in two limiting cases: either  $D=1$  or  $D=\infty$ . For example, the exact solution of the Hubbard model was given in  $D=1$  dimension by means of the Bethe-ansatz by Lieb and Wu<sup>1</sup>. The other class of exact solutions belongs to the other limiting case, i.e.  $D=\infty$ , when the dynamical mean-field approximation becomes exact<sup>2,3</sup>. The situation, however, gets more complicated as physically interesting, lower dimensional cases (e.g. systems in  $D=2$  or  $D=3$  dimensions) are considered.  $D>1$  rules out the applicability of the well-established Bethe-ansatz approach, while mean-field like descriptions lead to qualitatively or quantitatively incorrect conclusions, because the effects of spatial fluctuations are not taken properly into account<sup>4,5</sup>.

In recent years, some exact, *non-perturbative* methods have been developed to investigate the ground state of Hubbard and Hubbard-like models in large parameter regimes<sup>6-13</sup>. In the present work we focus on the so-called optimum ground state method (OGS) established by de Boer and Schadschneider<sup>12</sup>. Using this method one can obtain rigorous constraints on the model parameters which define regions where e.g. the CDW, the Néel, the fully saturated ferromagnetic, or the  $\eta$ -pairing state of momentum  $P$  becomes the exact ground state of the Hamiltonian.

The basic idea of the OGS method is to diagonalize a specially chosen local Hamiltonian and to tune all the model-parameters such a way that all local eigenstates which are needed to the construction of a given global ground state are also local ground states. This means that, on one hand, the corresponding eigenvalues of the local Hamiltonians should be all equal in magnitude and, on the other hand, this common value should be the lowest eigenvalue of the local problem. Following this method, one can obtain different regions in the parameter space of the model defined by inequalities. These inequalities mean *sufficient* conditions for a state to be the ground state inside a special region. Outside the derived region the state under study may or may not be the ground state of the model.

There are basically two different ways to enlarge the region of guaranteed stability: taking a larger local Hamiltonian or incorporating next-to-nearest neighbor interactions. As far as the first approach is concerned, it is obvious that the extent of local correlations which are taken into account is controlled by the size of the local Hamiltonian to be diagonalized exactly. Therefore, using local Hamiltonians defined on larger clusters of the lattice should typically lead to better constraints (i.e. extended stability regions), even if purely nearest neighbor interactions are present.

It is also well-known that next-to-nearest neighbor hopping has important effects. For instance, it was shown rigorously by Tasaki<sup>14</sup> that the pure Hubbard model characterized by hopping of electrons between nearest and next-to-nearest neighboring sites with dispersive bands exhibits ferromagnetism for finite Coulomb interaction at zero temperature. Recent Projection Quantum Monte Carlo studies by Hlubina *et al.*<sup>15</sup> confirmed this fact for finite temperatures, too. Beside the consequences of longer range hopping, the importance of nearest and next-to-nearest neighbor off-site interactions (both diagonal and off-diagonal) has also been emphasized both from experimental<sup>16</sup> and

from theoretical<sup>4,10,11,17,18</sup> sides. These extra terms (density-density type interaction, correlated hopping of electrons, hopping of electron pairs and the exchange coupling) all originate from the spin independent Coulomb interaction of electrons. Nevertheless, the values of these longer range interactions (e.g. between next-to-nearest neighboring sites) are known neither theoretically nor experimentally because of the complicated nature of screening processes in solids. However, it is obvious that these interactions are present in real materials. Their strength decreases with increasing interatomic distances on the lattice and they can have important effects on the characteristics of strongly correlated electron systems. Hence, it is a challenging task to incorporate and to treat them in an exact way on the level of the model Hamiltonian.

The aim of the present paper is two-fold. First, we would like to extend the previous calculations of Ref.<sup>12</sup> by choosing a larger local Hamiltonian which is defined on elementary plaquettes consisting of four lattice sites of the  $D$  dimensional hypercubic lattice. Using these local Hamiltonians and a simple, numerically exact method we have constructed the stability domains for the  $\eta$ -pairing states of momentum  $P = 0, \pi$  and for the fully saturated ferromagnetic state in the parameter space of an extended Hubbard model with a half-filled band. Given the size of the local Hamiltonian, the diagonalization is done numerically. The stability regions are deduced from the equality of the lowest eigenvalue of the chosen local Hamiltonian and of an upper bound derived appropriately from the variational principle of quantum mechanics. Second, the present choice of the larger local Hamiltonian gives us a simple way to incorporate next-to-nearest neighbor interactions, to treat them exactly and to investigate their effects on stability.

The paper is organized as follows: in Sec. II we introduce the method. In Sec. III the global Hamiltonian and the corresponding local Hamiltonian are defined. Sections IV A and IV B contain the stability domains in  $D=2, 3$  for the  $\eta$ -pairing states of momentum  $P$  and for the fully saturated ferromagnetic case, respectively. Finally a short summary and discussion closes the presentation in Sec. V.

## II. METHOD

Let us consider a model Hamiltonian defined on a discrete lattice. This (so-called global) Hamiltonian can be decomposed into the sum of equivalent local Hamiltonians  $h_{\text{cluster}}$  defined on identical clusters of lattice sites, the union of which covers the lattice. In other words

$$H = \sum_{\text{all clusters}} h_{\text{cluster}} . \quad (1)$$

If only on-site interactions are considered, each cluster might consist of a single lattice point and  $h_{\text{cluster}}$  is simply a Hamiltonian defined on the individual lattice points. If intersite interactions are also present, the cluster has to consist of (at least) two lattice sites (in case of only nearest neighbor interactions) and the proper *minimal* local Hamiltonian is actually a Hamiltonian defined on a bond joining two (in the simplest case nearest neighboring) sites. Nevertheless, the incorporation of longer and longer range interactions, or of more and more spatial correlations, requires the enlargement of the minimal cluster and hence the corresponding local Hamiltonian  $h_{\text{cluster}}$ . In principle, even infinite range interactions and correlations can be taken into account, but this would require  $h_{\text{cluster}} = H$ . The tractable cluster size is, however, limited by the feasibility of the necessary exact diagonalizations.

Setting up the local Hamiltonian and choosing a suitable local basis, the eigenvalue problem

$$h_{\text{cluster}}|\phi_{\text{cluster}}\rangle = \epsilon_{\text{cluster}}|\phi_{\text{cluster}}\rangle \quad (2)$$

can be solved exactly. Thus the full spectrum  $\epsilon_{\text{cluster}}^i$  ( $i = 1, \dots, \dim(h_{\text{cluster}})$ ) of  $h_{\text{cluster}}$  can be obtained. Since the clusters of decomposition are equivalent, the exact ground state energy  $E_{\text{GS}}$  is bounded from below by the relation

$$E_{\text{lower}} = N_{\text{cluster}} \min_i \epsilon_{\text{cluster}}^i \leq E_{\text{GS}} , \quad (3)$$

where the number of clusters on the considered lattice can be written as  $N_{\text{cluster}} = fL$ . Here  $f$  represents a simple combinatorial factor depending on the dimension and structure of the underlying lattice and  $L$  stands for the number of lattice sites.

The variational principle of quantum mechanics provides an upper bound for  $E_{\text{GS}}$ , namely

$$E_{\text{GS}} \leq \frac{\langle \Psi_{\text{trial}} | H | \Psi_{\text{trial}} \rangle}{\langle \Psi_{\text{trial}} | \Psi_{\text{trial}} \rangle} = E_{\text{upper}} , \quad (4)$$

where  $|\Psi_{\text{trial}}\rangle$  stands for an arbitrary trial wavefunction. In our case  $|\Psi_{\text{trial}}\rangle$  is an exact eigenstate of the global Hamiltonian for a certain set of model parameters.

Combining now Eqs. (3) and (4) yields

$$E_{\text{lower}} \leq E_{\text{GS}} \leq E_{\text{upper}} . \quad (5)$$

Exploiting that both  $E_{\text{lower}}$  and  $E_{\text{upper}}$  are analytic functions of the couplings of the global Hamiltonian, after carefully adjusting the coupling constants one can satisfy the equality

$$E_{\text{lower}} = E_{\text{upper}} \equiv E_{\text{GS}} , \quad (6)$$

which means that for a certain set of model parameters (in a special sector of the ground state phase diagram) the exact ground state energy  $E_{\text{GS}}$  is found. Furthermore, if the ground state has no degeneracy, the exact ground state  $|\Psi_{\text{GS}}\rangle$  of the global Hamiltonian is also found. In our case the non-degeneracy is provided by the fact that the states we consider (see Sec. IV) can be built up simply by using the lowest energy eigenstate of the local Hamiltonian. As an example let us consider the case of the  $D=1$  dimensional half-filled chain with bonds as clusters. For certain values of the coupling constants it can be reached that the non-degenerate lowest eigenvalue of the local Hamiltonian belongs to the parallel orientation of spins included on the bond. Since the bonds are equivalent, all the bonds along the chain contain parallel-oriented spins with the same local energy for the given set of model parameters. This fact yields the long range order of spins (here ferromagnetism) and also the non-degeneracy of the global ground state (apart from the spin-degeneracy). Similar arguments hold for the non-degeneracy of the ground state in higher dimensions, too.

Changing now the trial wavefunction and following the procedure discussed above a new ground state in a different region of the phase diagram can be found. Furthermore, repeating the method with more and more trial wavefunctions a large portion of the ground state phase diagram of the model can be explored.

### III. GLOBAL AND LOCAL HAMILTONIAN

Let us define now our global Hamiltonian on a  $D$  dimensional hypercubic lattice ( $D > 1$ ) in the following form

$$H_{\text{glob}} = U\hat{U} + \sum_{i,j} \left[ -t_{ij}\hat{t}_{ij} + X_{ij}\hat{X}_{ij} + V_{ij}\hat{V}_{ij} + Y_{ij}\hat{Y}_{ij} + J_{ij}\hat{J}_{ij} \right] - \mu\hat{\mu} , \quad (7)$$

where

$$\begin{aligned} \hat{U} &= \sum_i n_{i\uparrow}n_{i\downarrow} \\ \hat{t}_{ij} &= \sum_{\sigma} c_{i\sigma}^{\dagger}c_{j\sigma} \\ \hat{X}_{ij} &= \sum_{\sigma} c_{i\sigma}^{\dagger}c_{j\sigma} (n_{i,-\sigma} + n_{j,-\sigma}) \\ \hat{V}_{ij} &= \frac{1}{2} \sum_{\sigma,\sigma'} n_{i\sigma}n_{j\sigma'} \\ \hat{Y}_{ij} &= c_{i\uparrow}^{\dagger}c_{i\downarrow}^{\dagger}c_{j\downarrow}c_{j\uparrow} \\ \hat{J}_{ij} &= \frac{1}{2} \Delta_{ij}^{XY} (S_i^+S_j^- + S_j^+S_i^-) + \Delta_{ij}^Z S_i^z S_j^z \\ \hat{\mu} &= \sum_{i,\sigma} n_{i\sigma} . \end{aligned}$$

Here the fermion operators  $c_{i\sigma}^{\dagger}$  ( $c_{i\sigma}$ ) create (annihilate) electrons with spin  $\sigma$  in the single tight-binding Wannier orbital associated with site  $i$ .  $n_{i\sigma}$  is the particle number operator of electrons with spin  $\sigma$ , and  $n_i = n_{i\uparrow} + n_{i\downarrow}$ . Furthermore, the spin operators are given by  $S_i^+ = c_{i\uparrow}^{\dagger}c_{i\downarrow}$ ,  $S_i^- = c_{i\downarrow}^{\dagger}c_{i\uparrow}$  and  $S_i^z = \frac{1}{2}(n_{i\uparrow} - n_{i\downarrow})$ . The above Hamiltonian contains a term corresponding to the familiar Hubbard term of doubly occupied sites ( $U$ ), the hopping of a single electron (characterized by  $t_{ij}$ ), a density dependent (or correlated) hopping term ( $X_{ij}$ ), an intersite density-density type interaction of electrons ( $V_{ij}$ ), a term describing the hopping of electron pairs ( $Y_{ij}$ ), for  $\Delta_{ij}^{XY} = \Delta_{ij}^Z = 1$  a Heisenberg-type exchange interaction of spins ( $J_{ij}$ ) and a chemical potential term ( $\mu$ ). We note that  $\Delta_{ij}^{XY} = 0$  and  $\Delta_{ij}^Z = 1$  represents an Ising-type coupling of electron spins, while the case of  $\Delta_{ij}^{XY} = 1$  and  $\Delta_{ij}^Z = 0$  corresponds to an

XY-type interaction.  $J_{ij} > 0$  ( $J_{ij} < 0$ ) means antiferromagnetic (ferromagnetic) type of exchange. The relevance of the present model for real materials is discussed e.g. in Refs.<sup>4,20</sup>.

In the rest of the paper we investigate only couplings between on-site, nearest-neighbor and next-to-nearest neighbor electrons. Incorporating this restriction into Eq. (7) and using the convention  $A_l = A_{ij}$  ( $l=1, 2$  for  $i, j$  being nearest and next-to-nearest neighboring sites, respectively) for the intersite couplings, one can rewrite the global Hamiltonian as

$$\begin{aligned}
H_{\text{glob}} = & U \sum_{i=1}^L \left( n_{i\uparrow} - \frac{1}{2} \right) \left( n_{i\downarrow} - \frac{1}{2} \right) \\
& + \sum_{l=1}^2 \sum_{\langle ij \rangle_l} \left\{ \frac{1}{2} \sum_{\sigma} [X_l(n_{i,-\sigma} + n_{j,-\sigma}) - t_l] (c_{i\sigma}^{\dagger} c_{j\sigma} + c_{j\sigma}^{\dagger} c_{i\sigma}) + \frac{1}{2} V_l (n_i - 1)(n_j - 1) \right. \\
& \left. + \frac{1}{2} Y_l (c_{i\uparrow}^{\dagger} c_{i\downarrow}^{\dagger} c_{j\downarrow} c_{j\uparrow} + c_{j\uparrow}^{\dagger} c_{j\downarrow}^{\dagger} c_{i\downarrow} c_{i\uparrow}) + \frac{1}{2} J_{\text{xy}}^{(l)} (S_i^+ S_j^- + S_j^+ S_i^-) + J_z^{(l)} S_i^z S_j^z \right\} - \mu \hat{\mu} - E_0
\end{aligned} \tag{8}$$

Here  $\sum_{\langle ij \rangle_l}$  means a summation over nearest neighboring ( $l=1$ ) and next-to-nearest neighboring ( $l=2$ ) sites. The new notations  $J_{\text{xy}}^{(l)} = \Delta_l^{XY} J_l$  and  $J_z^{(l)} = \Delta_l^Z J_l$  are also used. In the special case of  $\Delta_l^{XY} = \Delta_l^Z = 1$ , however, the  $J_l \equiv J_{\text{xy}}^{(l)} = J_z^{(l)}$  notation will be kept for the sake of clarity.  $E_0$  represents a numerical constant which shifts the zero point of the energy scale. We remark that during the reformulation of Eq. (7) to Eq. (8) the chemical potential is also shifted by some constant.

Because we have only nearest and next-to-nearest neighbor interactions, the fully symmetric minimal clusters are the two-dimensional elementary plaquettes of the  $D=2$  dimensional square lattice, as depicted in Fig. 1. All  $D>2$  dimensional hypercubic lattices can be covered with the elementary plaquettes, however, in those cases the  $D$  dimensional hypercubes would be the fully symmetric minimal clusters.

Following the method of Sec. II the global Hamiltonian can be rewritten in terms of such plaquettes ( $\sum_{[i,j,l,m]}$  means a summation over the plaquettes) as

$$H_{\text{glob}} = \sum_{[i,j,l,m]} h_{ijlm} \tag{9}$$

with

$$\begin{aligned}
h_{ijlm} = & \frac{U}{z_2} \sum_{\alpha \in \mathcal{A}_0} \left( n_{\alpha\uparrow} - \frac{1}{2} \right) \left( n_{\alpha\downarrow} - \frac{1}{2} \right) \\
& + \frac{X_1}{4f_1} \sum_{(\alpha,\beta) \in \mathcal{A}_N} \sum_{\sigma} \left( c_{\alpha,\sigma}^{\dagger} c_{\beta,\sigma} + c_{\beta,\sigma}^{\dagger} c_{\alpha,\sigma} \right) (n_{\alpha,-\sigma} + n_{\beta,-\sigma}) \\
& + \frac{X_2}{f_2} \sum_{(\alpha,\beta) \in \mathcal{A}_{NN}} \sum_{\sigma} \left( c_{\alpha,\sigma}^{\dagger} c_{\beta,\sigma} + c_{\beta,\sigma}^{\dagger} c_{\alpha,\sigma} \right) (n_{\alpha,-\sigma} + n_{\beta,-\sigma}) \\
& - \frac{t_1}{4f_1} \sum_{(\alpha,\beta) \in \mathcal{A}_N} \sum_{\sigma} \left( c_{\alpha,\sigma}^{\dagger} c_{\beta,\sigma} + c_{\beta,\sigma}^{\dagger} c_{\alpha,\sigma} \right) - \frac{t_2}{f_2} \sum_{(\alpha,\beta) \in \mathcal{A}_{NN}} \sum_{\sigma} \left( c_{\alpha,\sigma}^{\dagger} c_{\beta,\sigma} + c_{\beta,\sigma}^{\dagger} c_{\alpha,\sigma} \right) \\
& + \frac{V_1}{4f_1} \sum_{(\alpha,\beta) \in \mathcal{A}_N} (n_{\alpha} - 1)(n_{\beta} - 1) + \frac{V_2}{f_2} \sum_{(\alpha,\beta) \in \mathcal{A}_{NN}} (n_{\alpha} - 1)(n_{\beta} - 1) \\
& + \frac{Y_1}{4f_1} \sum_{(\alpha,\beta) \in \mathcal{A}_N} \left( c_{\alpha\uparrow}^{\dagger} c_{\alpha\downarrow}^{\dagger} c_{\beta\downarrow} c_{\beta\uparrow} + c_{\beta\uparrow}^{\dagger} c_{\beta\downarrow}^{\dagger} c_{\alpha\downarrow} c_{\alpha\uparrow} \right) + \frac{Y_2}{f_2} \sum_{(\alpha,\beta) \in \mathcal{A}_{NN}} \left( c_{\alpha\uparrow}^{\dagger} c_{\alpha\downarrow}^{\dagger} c_{\beta\downarrow} c_{\beta\uparrow} + c_{\beta\uparrow}^{\dagger} c_{\beta\downarrow}^{\dagger} c_{\alpha\downarrow} c_{\alpha\uparrow} \right) \\
& + \frac{J_{\text{xy}}^{(1)}}{4f_1} \sum_{(\alpha,\beta) \in \mathcal{A}_N} \left( S_{\alpha}^+ S_{\beta}^- + S_{\beta}^+ S_{\alpha}^- \right) + \frac{J_{\text{xy}}^{(2)}}{f_2} \sum_{(\alpha,\beta) \in \mathcal{A}_{NN}} \left( S_{\alpha}^+ S_{\beta}^- + S_{\beta}^+ S_{\alpha}^- \right) \\
& + \frac{J_z^{(1)}}{2f_1} \sum_{(\alpha,\beta) \in \mathcal{A}_N} S_{\alpha}^z S_{\beta}^z + \frac{J_z^{(2)}}{f_2} \sum_{(\alpha,\beta) \in \mathcal{A}_{NN}} S_{\alpha}^z S_{\beta}^z - \frac{\mu}{z_2} \sum_{\alpha \in \mathcal{A}_0} n_{\alpha}
\end{aligned} \tag{10}$$

Here  $f_1 = z_2/z_1$  and  $f_2 = 2$  are numerical constants ( $z_1 = 2D$  and  $z_2 = 4\binom{D}{2}$ ) are the number of nearest and next-to-nearest neighboring sites, respectively, on the  $D$  dimensional hypercubic lattice). They are needed to avoid double

or higher counting of intersite interactions during the plaquette summation. Furthermore,  $t_1$ ,  $X_1$ ,  $V_1$ ,  $Y_1$  are the values of single electron hopping, correlated hopping, density-density type interaction and pair-hopping between nearest neighboring sites, respectively, while  $t_2$ ,  $X_2$ ,  $V_2$ ,  $Y_2$  indicate the analogous processes between next-to-nearest neighboring sites.  $U$  is the Hubbard interaction which can either be positive or negative in our model. To mimic real systems, however, it should be repulsive. In addition, spin interactions with exchange couplings  $J_{xy}^{(1)}$ ,  $J_{xy}^{(2)}$ ,  $J_z^{(1)}$  and  $J_z^{(2)}$  are included on the plaquette. Further notations:  $\mathcal{A}_0 = \{i, j, l, m\}$  means the set of individual lattice points,  $\mathcal{A}_N = \{(i, j), (j, l), (l, m), (m, i)\}$  represents the set of nearest neighboring sites and  $\mathcal{A}_{NN} = \{(i, l), (j, m)\}$  indicates the set of next-to-nearest neighboring sites on the plaquette (see Fig. 1). The possibility of anisotropies can be naturally incorporated into the local (and also global) Hamiltonian via the non-equivalence of the orthogonal directions of the plaquette. The effects, however, are not discussed in the present paper.

To apply Eq. (6) the connection between the number of lattice sites  $L$  and the number of clusters  $N_{\text{cluster}}$  (here plaquettes) is also needed. Combinatoric considerations give the following simple result for this quantity on a  $D$  dimensional hypercubic lattice,

$$N_{\text{cluster}} = \frac{1}{2}D(D-1)L. \quad (11)$$

## IV. RESULTS

As an illustration of the method described in Sec. II we consider a few physically interesting states, the  $\eta$ -pairing states of momentum  $P$  (Sec. IV A) which show off-diagonal long range order and are hence superconducting, and the fully saturated ferromagnetic state (Sec. IV B). We determine under what conditions these states are the ground states of the global Hamiltonian  $H_{\text{glob}}$ . All the calculations presented are done at half filling. Except the  $\eta$ -pairing state of momentum  $P=0$ , it is not possible to express the results in a compact analytic form as it has been done earlier in Ref.<sup>12</sup>. Therefore, and for the sake of visualization, we have restricted ourselves to special cuts of the parameter space in illustrating the effects of the larger local Hamiltonians and of next-to-nearest neighbor couplings. The cuts are chosen in such a way that the corresponding ground state phase diagrams can easily be compared with the previously published rigorous results of Strack *et al.*<sup>11</sup>, de Boer *et al.*<sup>12,24</sup> and Montorsi *et al.*<sup>25</sup>. In principle, one can also investigate the role of each nearest and next-to-nearest neighbor interactions separately, one by one, using our method.

### A. $\eta$ -pairing states of momentum $P$

The definition of the  $\eta$ -pairing operator of momentum  $P$  is given by the relation

$$\eta_P^\dagger = \sum_{j=1}^L e^{iPj} c_{j\downarrow}^\dagger c_{j\uparrow}^\dagger. \quad (12)$$

Using this operator an  $\eta$ -pairing state of momentum  $P$  and of pairs  $N$  can be constructed as

$$|\Psi_\eta(N, P)\rangle = K \left( \eta_P^\dagger \right)^N |0\rangle, \quad (13)$$

where  $K = \left[ \frac{(L-N)!}{L! N!} \right]^{\frac{1}{2}}$  is a normalization factor. For further details about the  $\eta$ -pairing states the reader is referred to the literature<sup>21–25</sup>. Since we would like the  $\eta$ -pairing states to be the ground state of our model, it is instructive to calculate the commutator of the  $\eta$ -operator with the global Hamiltonian  $H_{\text{glob}}$ . One finds that

$$\begin{aligned} [H, \eta_P^\dagger] = & \sum_{k=1}^2 \left[ \frac{1}{2} (X_k - t_k) \sum_{\langle jl \rangle_k} (e^{iPj} + e^{iPl}) (c_{j\downarrow}^\dagger c_{l\uparrow}^\dagger + c_{l\downarrow}^\dagger c_{j\uparrow}^\dagger) \right. \\ & \left. + \frac{1}{2} X_k \sum_{\langle jl \rangle_k} (e^{iPj} - e^{iPl}) \left[ (n_{l\uparrow} - n_{j\downarrow}) c_{l\downarrow}^\dagger c_{j\uparrow}^\dagger + (n_{l\downarrow} - n_{j\uparrow}) c_{j\downarrow}^\dagger c_{l\uparrow}^\dagger \right] \right] \end{aligned}$$

$$\begin{aligned}
& + \sum_{\langle jl \rangle_k} \left\{ \left( \frac{1}{2} Y_k e^{iPj} - U_k e^{iPl} \right) (n_j - 1) c_{l\uparrow}^\dagger c_{l\downarrow}^\dagger \right. \\
& \quad \left. + \left( \frac{1}{2} Y_k e^{iPl} - U_k e^{iPj} \right) (n_l - 1) c_{j\uparrow}^\dagger c_{j\downarrow}^\dagger \right\} - 2\mu\eta_P^\dagger.
\end{aligned} \tag{14}$$

Calculating now the quantity  $[H_{\text{glob}}, (\eta_P^\dagger)^N] |0\rangle$ , one can easily deduce the parameters where the  $\eta$ -pairing states of momentum  $P$  are the ground state of the starting model; for momentum  $P=0$  one arrives at the requirements  $X_i=t_i$  and  $Y_i=2V_i$  ( $i=1,2$ ), while for momentum  $P=\pi$  the conditions  $X_2=t_2$  and  $Y_i=(-1)^i 2V_i$  ( $i=1,2$ ) must be satisfied. One would also look for  $\eta$ -pairing states of momentum  $P \neq 0$  or  $P \neq \pi$ . These, however, represent the ground states of the global Hamiltonian in Eq. (7), where  $X_i=t_i$  ( $i=1,2$ ),  $U \leq -4t_1$  and all the other interaction constants are zero<sup>26,27</sup>.

Using the  $\eta$ -pairing states as trial wavefunctions, the upper bound in the thermodynamic limit for the ground state energy per lattice site  $L$  is

$$\frac{E_{\text{upper}}^{\eta_P}}{L} = \frac{1}{4}(U + z_1 V_1 + z_2 V_2) + \frac{1}{2}n\left(\frac{1}{2}n - 1\right) \sum_{l=1}^2 z_l V_l + \frac{1}{4}n\left(1 - \frac{1}{2}n\right) \sum_{l=1}^2 z_l Y_l \cos^l P - \mu n. \tag{15}$$

Exploiting the constraints between the amplitudes of pair-hopping  $Y_i$  and that of density-density type interaction  $V_i$  one gets for the half filled case ( $n=1$ ) that

$$E_{\text{upper}}^{\eta_P} = \frac{1}{4}L \left( U + \sum_{l=1}^2 z_l V_l \right) - \mu L. \tag{16}$$

Despite the fact, that the upper bounds for the  $\eta$ -pairing states of momentum  $P=0$  and  $P=\pi$  are identical, there is a characteristic difference between the two sets of wavefunctions; the state  $|\Psi_\eta(N, P=\pi)\rangle$  remains an exact eigenstate of the global Hamiltonian  $H_{\text{glob}}$  even if  $X_1 \neq t_1$ .

As mentioned earlier, it is possible to include more spatial correlations using local Hamiltonians defined on larger clusters of the lattice. This leads to the extension of the stability of the chosen state and means an improvement on the phase boundaries. For the  $\eta$ -pairing state of momentum  $P=0$  this effect is depicted in Fig. 2, where the  $\tilde{J}_{xy}$ - $\tilde{J}_z$  cut of the coupling constants' space is chosen. The inner triangle corresponds to the stability domain of the  $\eta_0$ -state determined by the OGS method of de Boer *et al.*<sup>12</sup> using bond Hamiltonians with purely nearest neighbor interactions. The shaded regions give the improvements of the boundaries applying our method with plaquette Hamiltonians containing only nearest neighbor interactions. The axes  $\tilde{J}_a = J_a^{(1)} A(U, V_1)$  ( $a=xy, z$ ) represent the rescaled values of nearest neighbor exchange interactions with the scaling factor of

$$A(U, V_1) = \left[ 2 \left| \frac{2U}{z_1} + V_1 \right| \right]^{-1}. \tag{17}$$

From Fig. 2 one can immediately read off the stability criteria for the  $\eta_0$ -state to be the ground state of  $H_{\text{glob}}$ . In the absence of next-to-nearest neighbor interactions (i.e.  $t_2=X_2=V_2=Y_2=J_2=0$ ) for  $V_1 \leq 0$  values of nearest neighbor density-density type interaction

$$\begin{aligned}
V_1 & \leq 0 \\
-1 & \leq \frac{\tilde{J}_z}{t_1} \leq -2 \left( \frac{\tilde{J}_{xy}}{t_1} \right)^2 + 1.
\end{aligned} \tag{18}$$

This is a considerable improvement over the  $V_1 \leq 0$ ,  $-1 \leq \tilde{J}_z/t_1 \leq -2|\tilde{J}_{xy}/t_1| + 1$  criteria derived following Ref.<sup>12</sup> using bond Hamiltonians.

If now next-to-nearest neighbor interactions are turn on, i.e. nonzero values of  $V_2$  (and hence  $Y_2$ ) are considered, the criteria of Eq. (18) remains valid in an improved form. In this case there is a need for the proper change of the scaling factor  $A$ , which now depends also explicitly on next-to-nearest neighbor interactions. The new value of the scaling factor is

$$A(U, V_1, V_2) = \left[ 2 \frac{z_2}{z_1} \left| \frac{2U}{z_2} + V_1 + V_2 \right| \right]^{-1}. \tag{19}$$

In real systems the  $X_1 = t_1$  requirement does not hold in general. However, the strengths of the corresponding two interactions are of the same magnitude. For  $X_1 \neq t_1$  only the  $\eta$ -pairing state of momentum  $P = \pi$  represents an exact eigenstate of the model Hamiltonian  $H_{\text{glob}}$ . Figure 3 shows the stability regions of the  $\eta_\pi$ -state for two different sets of model parameters expressed in units of  $eV$  in the  $U$ - $t_1$  plane. Dotted lines represent the boundary for stability regions corresponding to bond Hamiltonians, while solid lines are the boundaries calculated with plaquette Hamiltonians in the absence of next-to-nearest neighbor interactions. The shaded regions clearly show the extension of stability regimes due to the choice of larger local Hamiltonians.

We now consider the phase diagrams in the  $U$ - $Y_1$  (Fig. 4) and  $V_2$ - $V_1$  (Fig. 5) planes for fixed values of the other interactions. In Fig. 4 the exchange interaction has been fixed by the relation  $J_1 = -2Y_1$ . This assures that the global Hamiltonian of Sec. III coincides with the model Hamiltonian of Ref.<sup>25</sup>, where the authors, using the method of positive semi-definite operators<sup>8,10,11</sup>, derived rigorous bounds for the  $\eta_\pi$ -state. Comparing Fig. 4 with Fig. 1 in Ref.<sup>25</sup> two basic differences can be noticed. First, the boundary of the stability region, even for the special case of  $X_1 = t_1$ , varies with increasing values of nearest neighbor pair-hopping amplitude  $Y_1$  and has a maximum at  $Y_1 \approx 1.33t_1$ , instead of having a constant value. Second, the value of this maximum  $U_{\text{max}} \approx -0.33z_1t_1$  is independent of  $X_1$ . Furthermore, the stability regions for all values of  $X_1/t_1$  derived with the present method are always larger than the corresponding ones predicted by Montorsi *et al.*<sup>25</sup> and de Boer *et al.*<sup>12</sup> and exist for all positive values of  $Y_1$ . The relation  $Y_1 = -2V_1$  is also satisfied because the  $\eta_\pi$ -state has to be an exact eigenstate of the model. Therefore, the positivity of  $Y_1$  implies that the nearest neighbor density-density type interaction  $V_1$  has to be always negative, i.e. attractive, in order to find an  $\eta_\pi$  ground state.

As the  $\eta$ -pairing states consist of local pairs of electrons, it is of interest to investigate the effect of on-site Coulomb repulsion, characterized by  $U$ , on the stability of these pairs. To do this the  $V_2$ - $V_1$  plane is chosen at various values of  $U$ . As can be seen in Fig. 5 the local pairs are stable even in the presence of relatively large positive values of  $U$ . This requires, however, an attraction in the nearest neighbor density-density interaction channel. It should also be noted that the same type of interaction between next-to-nearest neighbors, denoted by  $V_2$ , can either be attractive or moderately repulsive. These findings lead us to the conclusion that the  $\eta$ -pairing state of momentum  $P = \pi$  remains the ground states of Eq. (7) even for positive values of the on-site Coulomb interaction. Hence superconductivity can exist in the extended Hubbard model with local repulsion ( $U > 0$ ), if a sufficiently strong nearest neighbor attraction ( $V_1 < 0$ ) is present.

The inclusion of next-to-nearest neighbor interactions increases remarkably the number of model parameters and hence the number of possible cuts of the parameter space. Therefore, we illustrate only some special, overall effects of these interactions. In order to model real systems all next-to-nearest neighbor interactions are chosen to be smaller in magnitude than the corresponding nearest neighbor ones. Nevertheless, the ratio of nearest to next-to-nearest neighbor interactions can be very different - it depends on the material. In Fig. 6 three plots are shown for different values of the couplings. These belong to the case of  $D = 2$ . The corresponding 3-dimensional plots display qualitatively the same features, except for the parameters of Fig. 6c. The quantitative discrepancy between the plots taken in  $D = 2$  and in  $D = 3$  is due to the fact that the number of next-to-nearest neighbors  $z_2$  is much larger in  $D = 3$  spatial dimensions than in  $D = 2$  on a hypercubic lattice. This suggests that in the framework of the present model the effects of next-to-nearest neighbor interactions are stronger in higher dimensions.

In Fig. 6a the stability region of the  $\eta$ -pairing state of momentum  $P = 0$  is shown for a certain set of model parameters in the absence (solid line) and in the presence (dotted line) of next-to-nearest neighbor couplings. One can notice the expansion of the stability region due to the presence of next-to-nearest neighbor interactions. Since a large value of  $|t_1|$  (in the presence of a fixed value of the nearest neighbor pair hopping  $Y_1$ ) favors the hopping of single electrons over the hopping of electron pairs, large values of  $|t_1|$  give rise to the breaking of local pairs. This means that the number of doubly occupied sites is not conserved any longer and, as a result, the  $\eta_0$ -state ceases to be the ground state of  $H_{\text{glob}}$ . In Fig. 6b the effects of next-to-nearest neighbor interactions on the stability of the  $\eta_\pi$ -state are shown. In contrast to the situation depicted in Fig. 6a no shrinking of the stability domain with increasing  $|t_1|$  can be observed. This can be explained with the different internal structure of the  $\eta_\pi$  pairs. In Fig. 6c we show a situation, where next-to-nearest neighbor couplings can either extend or shrink the stability region of the  $\eta_\pi$ -state. As mentioned earlier, the dimension of the lattice plays a crucial role here. In  $D = 2$  a huge portion of the  $U$ - $Y_1$  plane phase diagram is occupied by the  $\eta_\pi$ -state for any ratio of  $X_1/t_1$ . In  $D = 3$ , however, it was found for a wide parameter region that the  $\eta_\pi$ -state is the ground state of the model Hamiltonian  $H_{\text{glob}}$  only for the special case of  $X_1/t_1 = 1$ .

## B. The fully polarized ferromagnetic state

Let us consider now the fully ( $z$ -)polarized ferromagnetic state as the trial wave function defined as

$$|\Psi_{\text{FM}}\rangle = \prod_{j=1}^L c_{j\uparrow}^\dagger |0\rangle = \hat{F}|0\rangle. \quad (20)$$

Calculating the commutator of  $\hat{F}$  with  $H_{\text{glob}}$  one can see that this state is an exact eigenstate of the global Hamiltonian for any values of the interaction parameters. The trial wavefunction  $|\Psi_{\text{FM}}\rangle$  yields in the thermodynamic limit at half-filling the upper bound

$$E_{\text{upper}}^{\text{FM}} = -\frac{1}{4}UL + \frac{1}{8}L \sum_{l=1}^2 z_l J_z^{(l)} - \mu L \quad (21)$$

for the ground state energy.

In what follows, we reveal under what conditions Eq. (20) is the ground state of  $H_{\text{glob}}$ . For the sake of simplicity we concentrate on a fixed set of numerical values of nearest neighbor couplings, as it has already been estimated by Hubbard<sup>28</sup> for electrons in  $d$ -bands of transition metals. The values of next-to-nearest neighbor interactions are chosen to be fractions of the corresponding nearest neighbor ones. The ratio of nearest to next-to-nearest neighbor couplings is set to be about 5-8. We think this range of ratio to be appropriate for a wide class of materials. Furthermore, this is in agreement with the work of Appel *et al.*<sup>29</sup> who also made quantitative predictions regarding the strength of nearest and next-to-nearest neighbor correlated hopping  $X_1$  and  $X_2$ , respectively. Further calculations at different sets of model parameters have also shown that the phase diagrams plotted in Figs. 7, 8 and 9 are generic. This suggests that the above choice of model parameters captures the essential physics.

In Fig. 7 we present the changes in the stability domain induced by using plaquette Hamiltonians. For comparison with the corresponding result of Ref.<sup>12</sup> with bond Hamiltonians, the plaquette Hamiltonians contained no next-to-nearest neighbor interactions. The shaded region shows the enlargement in the stability domain of the fully saturated ferromagnetic state. As can be seen from the figure, there is a reasonable extension with respect to  $t_1$ . While in the case of bond Hamiltonians the value of the correlated hopping  $X_1$  should be very close in magnitude to  $t_1$  in order to reach the boundary of the stability region at  $U_{\text{min}} \approx 4 \text{ eV}$ , we have a much broader region for that using plaquette Hamiltonians. The broadening implies that the additionally incorporated spatial correlations really lead to the stabilization of the ordered phase, in our case the ferromagnetism.

The global Hamiltonian  $H_{\text{glob}}$  containing purely nearest neighbor interactions can be transformed into an effective Heisenberg model in the large- $U$  limit at half filling (see e.g. Kollar *et al.*<sup>30</sup> and references therein) with the effective exchange coupling of

$$J_{\text{eff}} = \frac{t_1^2}{U} \left(1 - \frac{X_1}{t_1}\right)^2 + J_1. \quad (22)$$

This favors ferromagnetism for all  $J_{\text{eff}} < 0$ . Neglecting in Eq. (7) all intersite interactions but the nearest neighbor exchange interaction, the latter equation suggests a simple perturbative criterion for the stability of ferromagnetism in the large- $U$  limit; ferromagnetism is favored over antiferromagnetism for all  $U > U_c = t_1^2/|J_1|$  (note that in Eq. (7)  $J_1 = -|J_1| < 0$  means the ferromagnetic coupling). It is known that the OGS approach using bond Hamiltonians gives the criterion  $U/z_1 > U_c$  as the stability requirement in the same regime. Therefore it possibly underestimates the stability of the fully polarized ferromagnetic state. Taking into account larger local Hamiltonians defined on elementary plaquettes of the hypercubic lattice one gets the criterion  $U/z_1 > U_c/2$  for the stability, which means more extended stability domain in the large- $U$  limit. Furthermore, it suggests that (at least in the large- $U$  limit) the stability criterion has the form of  $U > \frac{2}{b}U_c$ , where  $b$  is the function of the size of the cluster on which the local Hamiltonian is defined. The possible scaling behavior of the stability criterion and the concrete form of  $b(N_{\text{cluster}})$  are discussed elsewhere<sup>31</sup>.

Since the fully polarized ferromagnetic state at half filling is an exact eigenstate of  $H_{\text{glob}}$  we have got no *a priori* restrictions for the values of the interaction parameters. The extensive calculations, however, lead to a simple restriction between  $J_{xy}^{(1)}$  and  $J_z^{(1)}$ . In order to have a ferromagnetic ground state of a model containing spin interactions which vary continuously from a Heisenberg-type interaction to a simple Ising-type one, the  $-1 < \Delta_1^{XY} \leq 1$  requirement must hold. This means that the restriction

$$-|J_z^{(1)}| \leq -J_{xy}^{(1)} < |J_z^{(1)}| \quad (23)$$

has to be always satisfied. In Fig. 8 the consequence of Eq. (23) is illustrated in the  $U$ - $t_1$  cut of the parameter space at  $\Delta_1^Z = 1$  and  $J_z^{(1)} = -|J_z^{(1)}| < 0$  for various values of  $\Delta_1^{XY}$ . The size of the stability region is maximal at  $\Delta_1^{XY} = 1$  and gradually decreases as  $\Delta_1^{XY}$  reaches  $\Delta_1^{XY} = -1$ . Any further decrease of  $\Delta_1^{XY}$  yields that our ferromagnetic state



which is fully  $z$ -polarized is no longer the ground state of  $H_{\text{glob}}$ ; for  $J_{\text{xy}}^{(1)} = J_z^{(1)}$   $H_{\text{glob}}$  is  $\text{SU}(2)$  symmetric which implies the degeneracy of the ground state with respect to  $\text{SU}(2)$  rotations. For anisotropic exchange couplings favouring the  $xy$ -plane, the ground state polarization may still be macroscopic, however, it no longer points in the  $z$ -direction. This means that the fully  $z$ -polarized ferromagnetic trial wavefunction becomes unstable. We note that Eq. (23) must hold even in the presence of next-to-nearest neighbor couplings.

In Fig. 9 the effects of nonzero next-to-nearest neighbor hopping  $t_2$  are illustrated for a fixed set of model parameters, first in the  $U$ - $t_1$  plane [plot (a), in units of  $eV$ ] and second in the  $U$ - $t_2$  plane [plot (b), in units of  $t_1$ ]. In Fig. 9a the dotted line represents the phase boundary in the absence of next-to-nearest neighbor interactions while solid, long-dashed, dashed and dotted-dashed lines correspond to phase boundaries in the presence of next-to-nearest neighbor interactions for various values of  $t_2$ . As can be seen from the plot, next-to-nearest neighbor interactions can help in stabilizing ferromagnetism for the chosen set of model parameters as long as  $t_2/t_1$  has a small, positive value. For negative or large positive values of  $t_2/t_1$ , however, the stability domain reduces significantly and stronger Coulomb repulsion is needed for the stabilization. This means e.g. that for a reasonably narrow band ( $t_1 \approx 0.4 \text{ eV}$ ) with the ratio of  $t_2/t_1 = 0.1$ , the required minimal stabilizing Coulomb repulsion is about  $U_{\text{min}} \approx 3 \text{ eV}$ . The same value of  $U$  at  $t_2/t_1 = -0.25$  is about  $U_{\text{min}} \approx 30 \text{ eV}$  which is a magnitude larger. Nevertheless, the above range of Coulomb interactions can be considered reasonable for real materials.

In Fig. 9b the effects of change in non-interacting dispersion due to the inclusion of next-to-nearest neighbor hopping are shown for a square (solid line) and for a cubic (dotted line) lattice. The stability domains of ferromagnetism depend on the dimensionality of the lattice and do not coincide. It is interesting to note that the most favorable values of  $t_2/t_1$  for which the Coulomb interaction takes its minimal value  $U_{\text{min}}$  also depend on the spatial dimension. The shapes of the stability domains are also of interest: in a well-defined region of  $t_2/t_1$   $U_{\text{min}}$  changes only by a slight amount but as soon as the edges of this region are reached  $U$  increases drastically. This feature suggests that inside the stability regions a nonzero next-to-nearest neighbor hopping via the asymmetric density of states<sup>13,32</sup> helps (in the presence of other next-to-nearest neighbor interactions) in stabilizing ferromagnetism but outside it destabilizes ferromagnetic ordering. The edges are determined mainly by the dispersions (hence the shape of the particular density of states) and tuned further by other interactions being present in  $H_{\text{glob}}$ .

It is also known that the inclusion of nearest neighbor ferromagnetic exchange interaction in the pure Hubbard model favors the parallel ordering of electron spins<sup>4,11,19</sup>. In Fig. 10 we considered the pure Hubbard model supplemented with next-to-nearest neighbor hopping  $t_2$  and nearest and next-to-nearest neighbor exchange interactions  $J_1$  and  $J_2$ , respectively. All the other type of couplings are turned off. As can be seen in the figure, the stability domain of ferromagnetism extends with increasing value of the Coulomb repulsion and in the limit of  $U \rightarrow \infty$  fills the whole  $J_1, J_2 \leq 0$  quarter of the phase diagram. The fully polarized ferromagnetic state remains the ground state of Eq. (7) for finite values of  $U$  only in the presence of finite values of  $J_1$  and  $J_2$ . Figure 10 also shows that the required minimal values of  $|J_2|$  are about an order of magnitude less than the required minimal values of  $|J_1|$ , and  $J_2$  should also be ferromagnetic in nature, i.e.  $J_2 < 0$ .

## V. CONCLUSIONS

In the present paper we have studied in the thermodynamic limit the ground state phase diagram of the Hubbard model supplemented by nearest and next-to-nearest neighbor interactions. The purpose of the study was to clarify to what extent and in which way the inclusion of additional spatial correlations changes the stability of physically interesting states, the  $\eta$ -pairing state of momentum  $P = 0$  and  $P = \pi$ , or the fully  $z$ -polarized ferromagnetic state. The phase boundaries are extracted from the equality of an upper and a lower bound of the ground state energy, hence these are exact. The additional spatial correlations are introduced via the computation of the lower bound on elementary plaquettes, instead of bonds, of the  $D$  dimensional hypercubic lattice. Except the case of  $\eta$ -pairing state of momentum  $P = 0$  the exact phase boundaries cannot be given in closed, analytic forms. Instead, they are shown graphically in special cuts of the parameter space of the model under study.

The phase boundaries presented are *sufficient* phase boundaries. This means that outside the region defined by the exact conditions a certain state might remain the ground state of the model. Diagonalizing local Hamiltonians defined on larger clusters of the lattice the phase boundaries might be further improved. This improvement with increasing cluster size addresses a further issue: does the stability domain of a given ordered phase extend further with taking larger and larger clusters, or is there a convergence regarding the location of its phase boundary? If the latter holds, we could determine the phase boundaries with a simple extrapolation even in the limit of  $H = h_{\text{cluster}}$ . Based on preliminary results we believe that the further extension of stability domains decreases rapidly with increasing cluster size. For instance, computing the lower bounds of the ground state energy with diagonalizing local Hamiltonians defined on clusters of 6 lattice sites, the further expansion of the stability regions is only about a few percentage,

generally 4-5 % or less.

Considering the effects of more spatial correlations, which was equivalent in our case with the choice of plaquette Hamiltonians, we have improved significantly the previously derived rigorous results of Refs.<sup>11,12,24,25</sup>. This means e.g. for the fully polarized ferromagnetic state that the minimal value of the Coulomb repulsion required to stabilize ferromagnetism along reasonable values of nearest neighbor interactions is predicted to be about 6-10 eV (in  $D=3$ ) in a relatively broad range of nearest neighbor hopping (see Fig. 7).

Another goal of the present study was to determine the overall effects of next-to-nearest neighbor interactions on the stability domains. The inclusion of next-to-nearest neighbor interactions can be done naturally using plaquette Hamiltonians. Up to our knowledge, the effects of next-to-nearest neighbor interactions, except those of next-to-nearest neighbor hopping, have not yet been considered rigorously in the literature. The relative strengths of next-to-nearest neighbor interactions are much smaller than that of nearest neighbor interactions, the stability conditions, however, strongly depend on them. Their effect in various sectors of the phase diagram is different and they result either an extension or a shrinking of the stability domain. For instance, taking the  $\eta$ -pairing state of momentum  $P = \pi$  the possible maximal value of the Coulomb repulsion  $U_{\max}$ , up to which the  $\eta_\pi$ -state remains the ground state of the extended Hubbard model (i.e. the model has a superconducting ground state), is increased from 6 eV to 8-9 eV (in  $D=3$ ) by the inclusion of relatively small next-to-nearest neighbor interactions (Fig. 6b).

It is also known that next-to-nearest neighbor hopping of single particles, which is characterized by the hopping amplitude  $t_2$ , is of importance in real materials. Our results are in good agreement with this fact. We showed that  $t_2$  has a characteristic effect e.g. on the stability of the fully saturated ferromagnetic state. Even a small ratio of  $t_2/t_1$ , i.e. a small amount of frustration in the dispersion, introduces a qualitative change into the phase diagram. The change is mostly a shrinking of the stability domain, however, for small ratios ( $t_2/t_1 \leq 0.15$ ) the presence of  $t_2$  helps in stabilizing ferromagnetism (Fig. 9). This is in good agreement with recent DMRG studies taken on 1-dimensional triangular lattice<sup>33</sup>. It is interesting to note that in our calculations the extension of ferromagnetic domain occurs always at positive ratios of  $t_2/t_1$  for fixed values of the other parameters of the model.

The Hubbard model supplemented only by exchange interactions  $J_1$  and  $J_2$  has also been investigated. Our results are in good agreement with Ref.<sup>34</sup>, i.e. the critical values of nearest and next-to-nearest exchange interactions to give rise to ferromagnetism approach zero as  $U \rightarrow \infty$  in the case of a half-filled band in any dimensions. However, at finite values of the Coulomb repulsion  $J_1$  and  $J_2$  should also be finite, if the ground state is the fully polarized ferromagnetic state.

In summary, we have established a simple method which allows us to incorporate and to treat the effects of next-to-nearest neighbor correlations and interactions in an *exact* fashion. We showed that the ground state of the extended Hubbard model in the thermodynamic limit at half filling is superconducting or ferromagnetic, depending on the interaction strengths. The improved phase boundaries for certain sets of model parameters have also been constructed.

## VI. ACKNOWLEDGEMENTS

The author would like to thank Zs. Gulácsi and E. Müller-Hartmann for their continuous encouragement during the present work. He also thanks A. Schadschneider, F. Pázmándi, G. Uhrig and P. Würth for valuable discussions and careful reading of the manuscript. The author is gratefully acknowledges financial support of Deutscher Akademischer Austauschdienst (DAAD) and the hospitality of the University of Cologne, Germany.

---

<sup>a</sup> Postal address: Ormós L. u. 3, H-4032 Debrecen, Hungary.

<sup>1</sup> E.H. Lieb and F.Y. Phys. Rev. Lett. **20**, 1445 (1968).

<sup>2</sup> W. Metzner and D. Vollhardt, Phys. Rev. Lett. **62**, 324 (1989).

<sup>3</sup> E. Müller-Hartmann, Z. Phys. B **74**, 507 (1989); *ibid.* **76**, 211 (1989).

<sup>4</sup> J.C. Amadon and J.E. Hirsch, Phys. Rev. **B54**, 6364 (1996).

<sup>5</sup> M. Ulmke, Eur. Phys. J. B **1**, 301 (1998).

<sup>6</sup> F.H.L. Essler, V.E. Korepin and K. Schoutens, Phys. Rev. Lett. **70**, 73 (1993).

<sup>7</sup> A.A. Ovchinnikov, J. Phys. **CM6**, 11057 (1994).

<sup>8</sup> U. Brandt and A. Gieseckus, Phys. Rev. Lett. **68**, 2648 (1992).

<sup>9</sup> A. Mielke and H. Tasaki, Comm. Mat. Phys. **158**, 341 (1993).

<sup>10</sup> R. Strack and D. Vollhardt, Phys. Rev. Lett. **70**, 2637 (1993).

- <sup>11</sup> R. Strack and D. Vollhardt, Phys. Rev. Lett. **72**, 3425 (1994).
- <sup>12</sup> J. de Boer and A. Schadschneider, Phys. Rev. Lett. **75**, 4298 (1995).
- <sup>13</sup> T. Hanisch, G.S. Uhrig and E. Müller-Hartmann, Phys. Rev. **B56**, 13960 (1997).
- <sup>14</sup> H. Tasaki, Phys. Rev. Lett. **75**, 4678 (1995).
- <sup>15</sup> R. Hlubina, S. Sorella and F. Guinea, Phys. Rev. Lett. **78**, 1343 (1997).
- <sup>16</sup> C. Verdozzi and M. Cini, Phys. Rev. **B51**, 7412 (1995).
- <sup>17</sup> J. van den Brink *et al.*, Phys. Rev. Lett. **75**, 4658 (1995).
- <sup>18</sup> Zs. Szabó and Zs. Gulácsi, Phil. Mag. **B76**, 911 (1997).
- <sup>19</sup> J.E. Hirsch, Phys. Rev. **B56**, 11022 (1997).
- <sup>20</sup> M. Kollar, R. Strack and D. Vollhardt, Phys. Rev. **B53**, 9225 (1996).
- <sup>21</sup> C.N. Yang, Rev. Mod. Phys. **34**, 694 (1962).
- <sup>22</sup> C.N. Yang, Phys. Rev. Lett. **63**, 2144 (1989).
- <sup>23</sup> S.-Q. Shen and Z.-M. Qiu, Phys. Rev. Lett. **71**, 4238 (1993).
- <sup>24</sup> J. de Boer, V.E. Korepin and A. Schadschneider, Phys. Rev. Lett. **74**, 789 (1995).
- <sup>25</sup> A. Montorsi and D.K. Campbell Phys. Rev. **B53**, 5153 (1996).
- <sup>26</sup> A.A. Aligia and L. Arrachea, Phys. Rev. Lett. **73**, 2240 (1994).
- <sup>27</sup> A. Schadschneider, Phys. Rev. **B51**, 10386 (1995).
- <sup>28</sup> J. Hubbard, Proc. R. Soc. London A **276**, 238 (1963).
- <sup>29</sup> J. Appel, M. Grodzicki and F. Paulsen, Phys. Rev. **B47**, 2812 (1993).
- <sup>30</sup> D. Vollhardt *et al.*, Z. Phys. B **103**, 283 (1997).
- <sup>31</sup> Zs. Szabó, *in preparation*
- <sup>32</sup> J. Wahle *et al.*, Phys. Rev. **B58**, 12749 (1998).
- <sup>33</sup> R. Arita, Y. Shimoi, K. Kuroki and H. Aoki, Phys. Rev. **B57**, 10609 (1998).
- <sup>34</sup> J.E. Hirsch J. Appl. Phys. **67**, 4549 (1990).

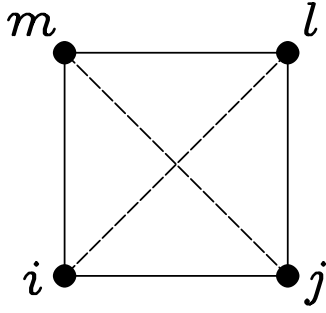


FIG. 1. An elementary plaquette of the  $D = 2$  dimensional square lattice. Solid lines represent different types of nearest neighbor couplings while dashed lines symbolize the next-to-nearest neighbor ones. The local Hamiltonian is defined on this cluster.

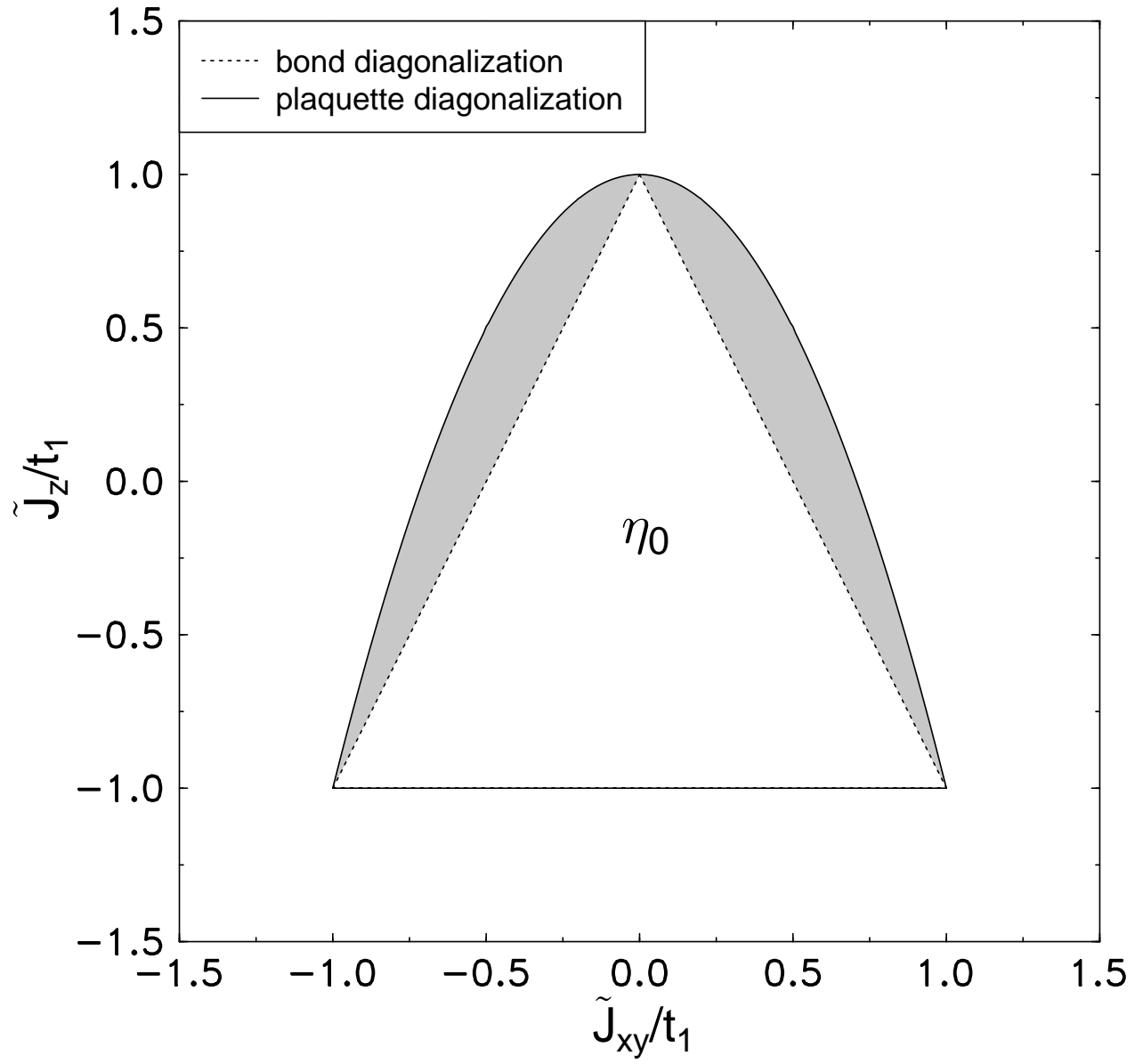


FIG. 2. Exact stability region of  $\eta$ -pairing state of momentum  $P=0$  ( $\eta_0$ ) at half filling. The shaded region represents the enlargement of the stability domain due to the choice of local Hamiltonian defined on elementary plaquettes (see Fig. 1) of the lattice. All the next-to-nearest neighbor interactions are kept zero.

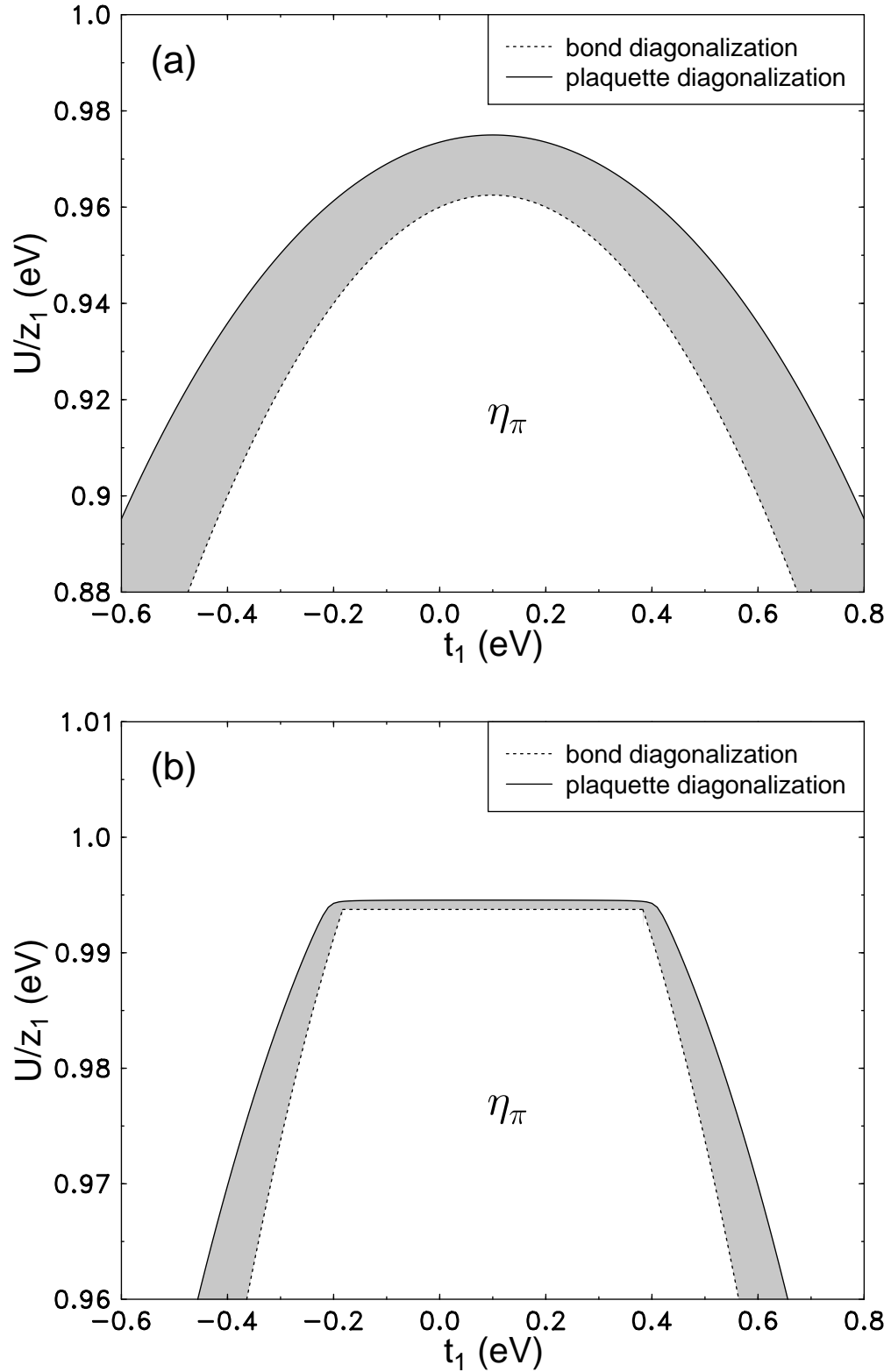


FIG. 3. Exact stability domains of  $\eta$ -pairing state of momentum  $P=\pi$  ( $\eta_\pi$ ) at half filling for two different sets of nearest neighbor couplings in the absence of next-to-nearest neighbor interactions [plot (a):  $X_1=0.1$  eV,  $V_1=-2$  eV and  $J_1=0.05$  eV; plot (b):  $X_1=0.1$  eV,  $V_1=-2$  eV,  $J_{xy}^{(1)}=-0.02$  eV and  $J_z^{(1)}=-0.015$  eV]. The shaded regions represent the enlargement of the stability domain due to the choice of local Hamiltonian defined on plaquettes instead of bonds.

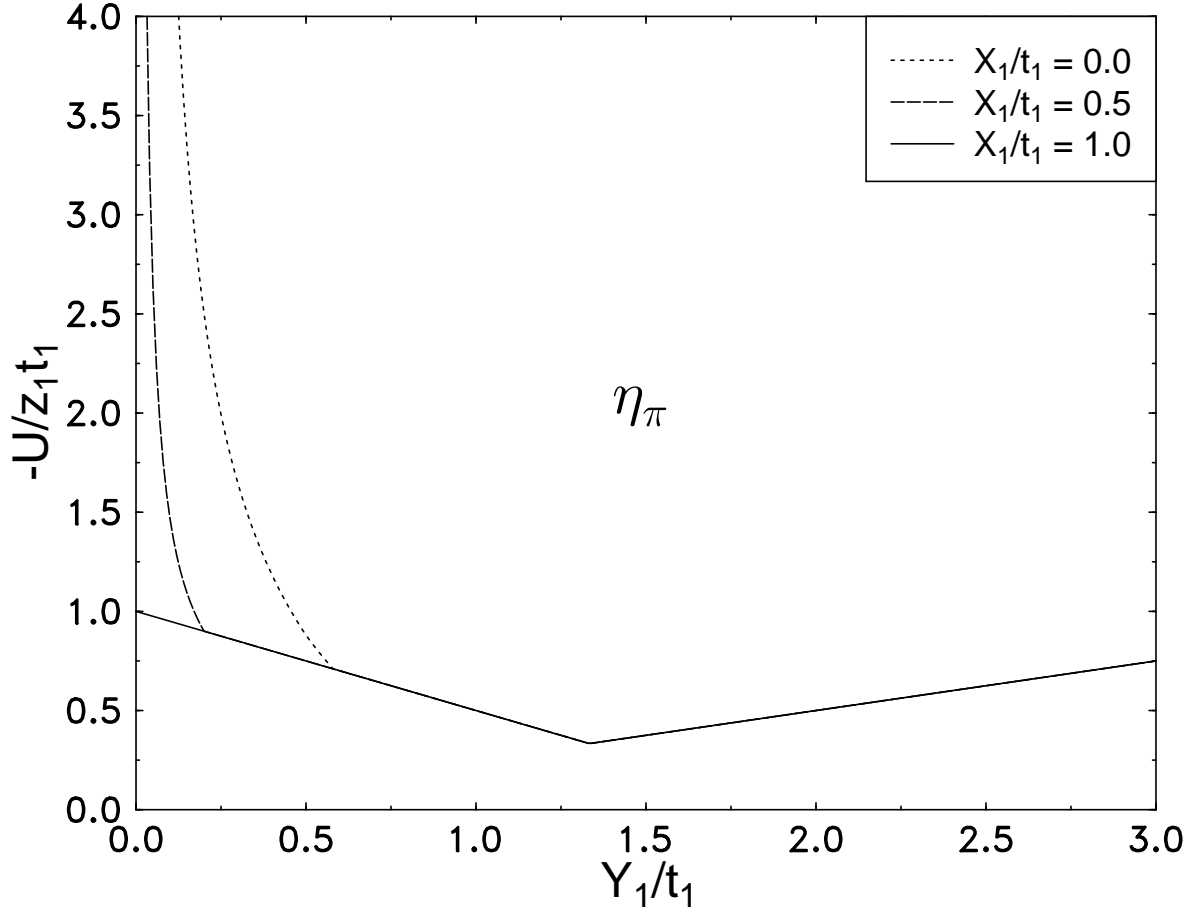


FIG. 4. Effects of correlated hopping  $X_1$  and pair hopping  $Y_1$  on the stability of  $\eta$ -pairing state of momentum  $P = \pi$  ( $\eta_\pi$ ). Each next-to-nearest neighbor interaction is turned off. We note, that beyond a well-defined value of  $Y_1$  the phase boundaries for the cases  $X_1 \neq t_1$  and  $X_1 = t_1$  coincide.

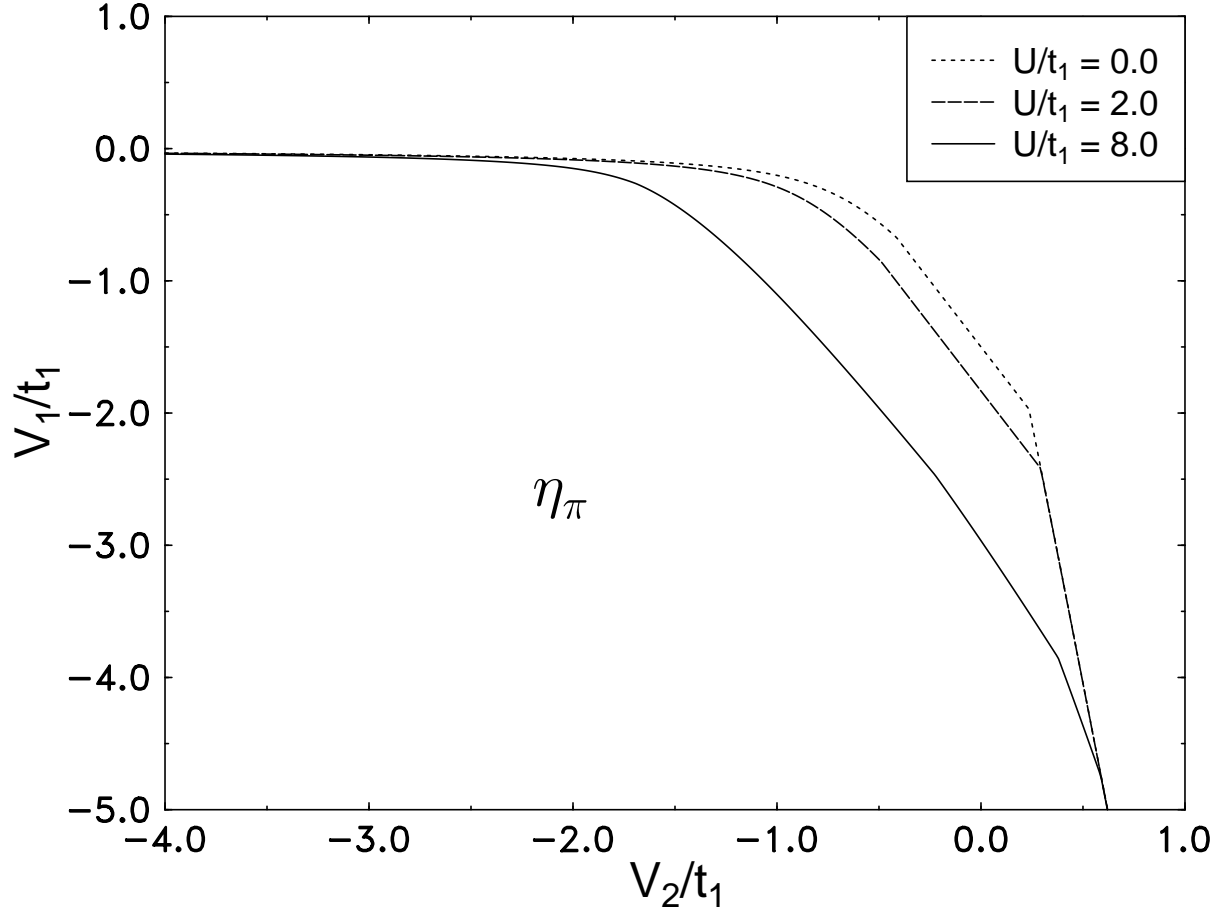


FIG. 5. Stability domains of  $\eta$ -pairing state of momentum  $P=\pi$  ( $\eta_\pi$ ) in  $D=3$  in the presence of various on-site Coulomb repulsions and intersite density-density type interactions ( $V_1, V_2$ ). The remaining parameters of Eq. (7) are chosen as follows:  $t_2 = -\frac{1}{4}t_1$  and  $X_1 = J_1 = J_2 = 0$ . Note, that  $X_2, Y_1$  and  $Y_2$  are uniquely fixed via the rigorous restrictions derived earlier in order that Eq. (13) be an exact eigenstate. In  $D=2$  similar stability regions emerge.



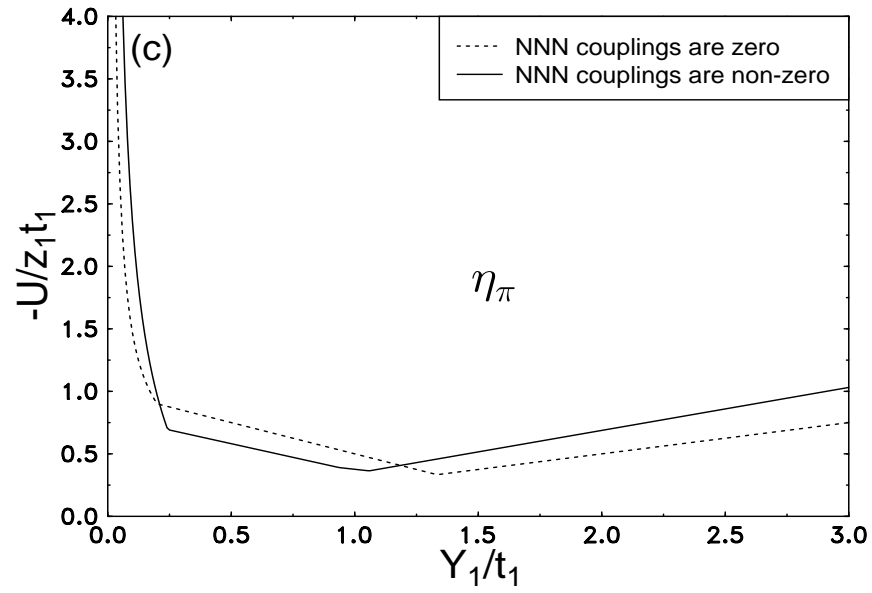
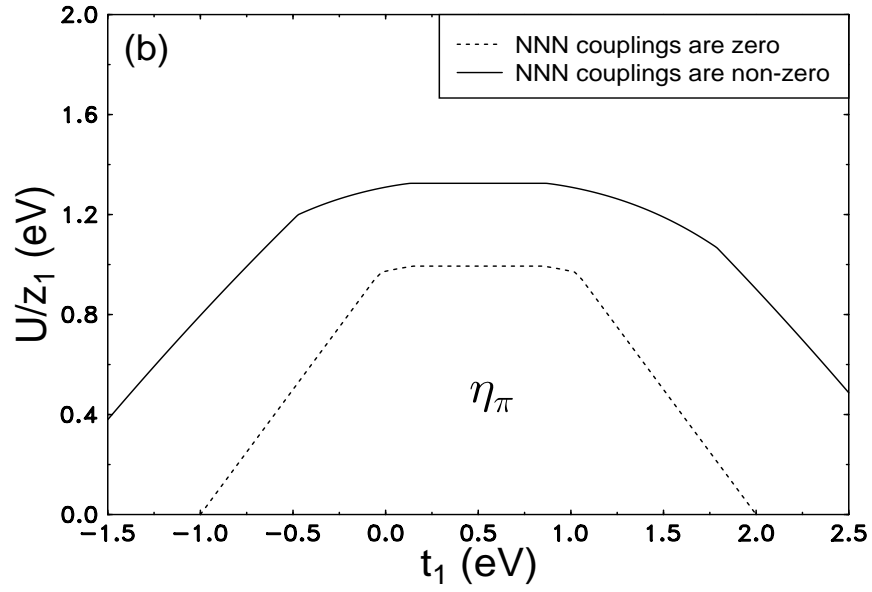
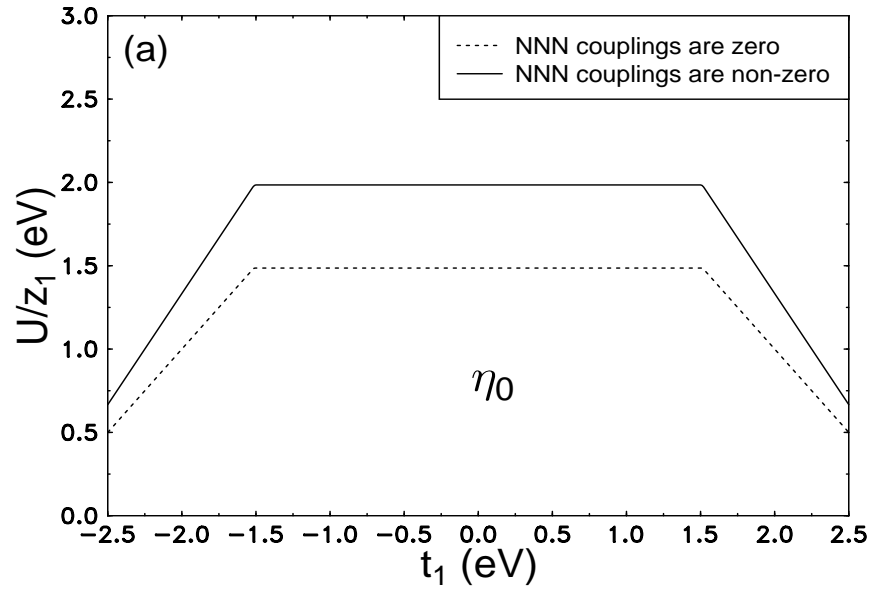


FIG. 6. Effects of next-to-nearest neighbor (NNN) couplings on the stability of  $\eta$ -pairing states of momentum  $P$  on a two dimensional square lattice. The values of the interaction constants are fixed as follows; plot (a):  $P = 0$ ,  $V_1 = -3$  eV,  $J_{xy}^{(1)} = \frac{1}{40}$  eV,  $J_z^{(1)} = \frac{1}{30}$  eV,  $t_2 = \frac{1}{3}t_1$ ,  $V_2 = \frac{1}{3}V_1$  and  $J_a^{(2)} = \frac{1}{3}J_a^{(1)}$  (a=xy,z); plot (b):  $P = \pi$ ,  $V_1 = -2$  eV,  $X_1 = 0.5$  eV,  $J_{xy}^{(1)} = -\frac{1}{50}$  eV,  $J_z^{(1)} = -\frac{1}{40}$  eV,  $t_2 = -\frac{1}{3}t_1$ ,  $V_2 = \frac{1}{3}V_1$  and  $J_a^{(2)} = \frac{1}{3}J_a^{(1)}$  (a=xy,z); plot (c):  $P = \pi$ ,  $X_1 = \frac{1}{2}t_1$ ,  $J_1 = -2Y_1$ ,  $t_2 = -\frac{1}{5}t_1$ ,  $Y_2 = \frac{1}{8}Y_1$  and  $J_2 = \frac{1}{8}J_1$ .

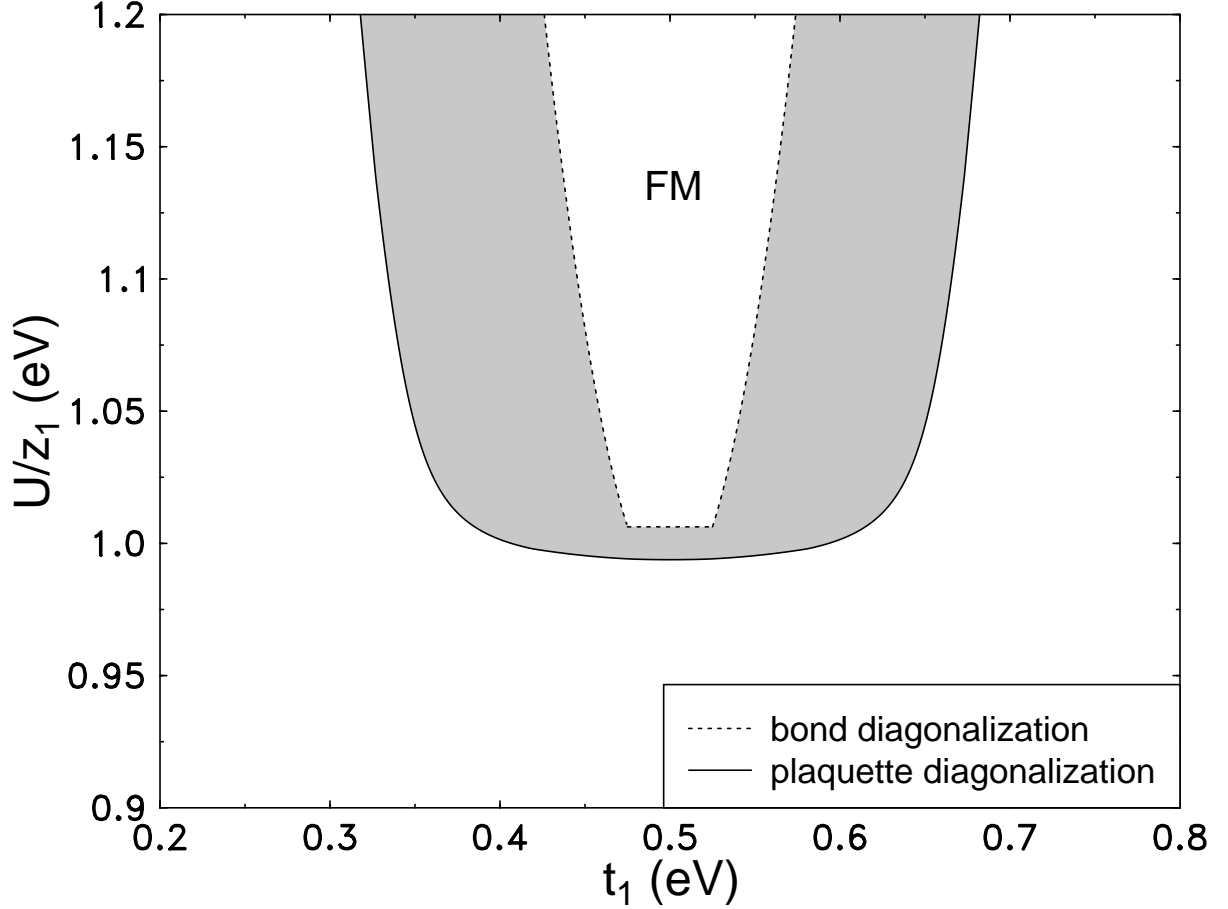


FIG. 7. Exact stability region for the fully saturated ferromagnetic state (FM) at half filling on a  $D$  dimensional hypercubic lattice for a certain set of model parameters  $X_1 = 0.5$  eV,  $V_1 = 2$  eV and  $Y_1 = -J_1 = \frac{1}{40}$  eV in the absence of next-to-nearest neighbor interactions. The shaded region represents the extension of the stability of the fully saturated ferromagnetic state as the ground state of Eq. (7) due to the choice of local Hamiltonian defined on elementary plaquettes, instead of bonds, of the lattice.

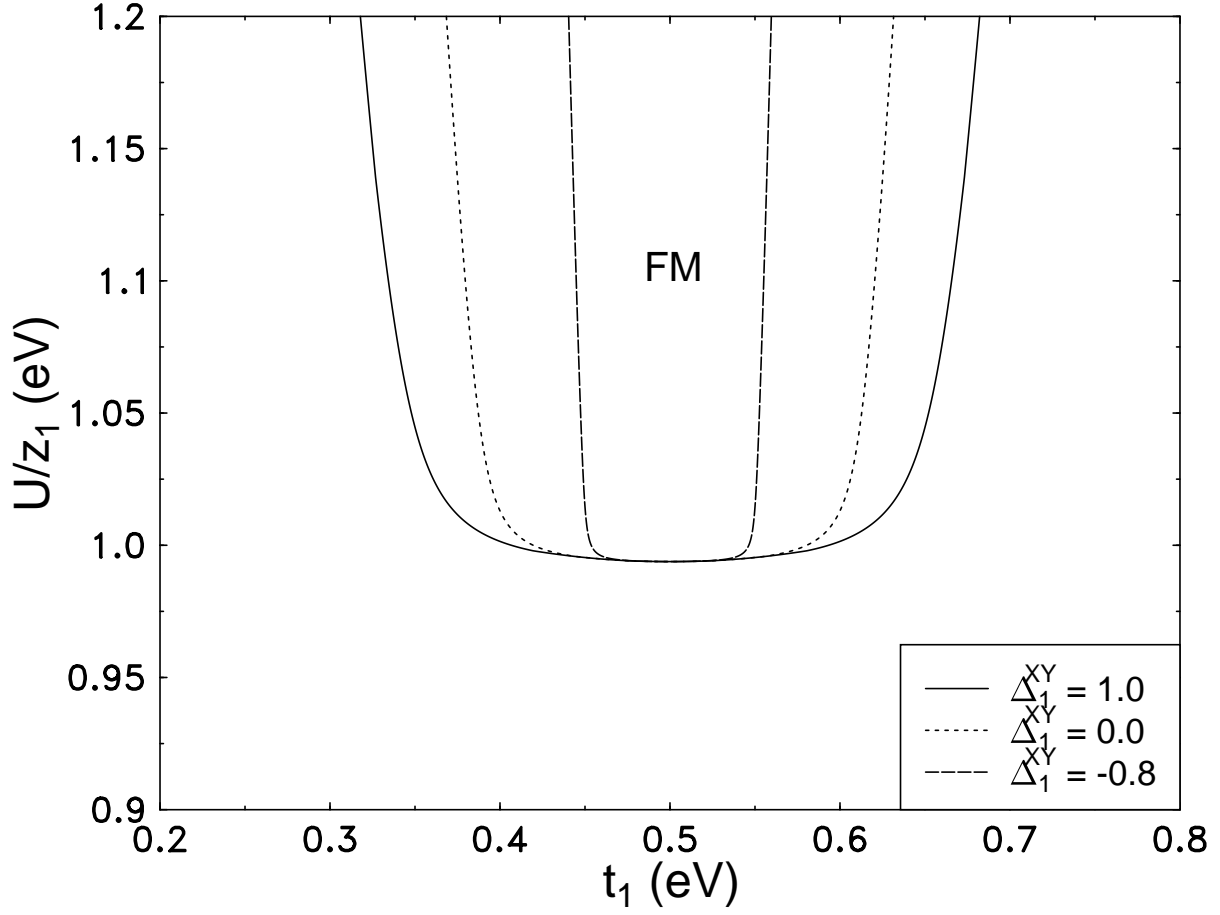


FIG. 8. Stability regions of the fully saturated ferromagnetic state (FM) for various values of  $\Delta_1^{XY}$ . The stability region is maximal at  $\Delta_1^{XY} = 1$  and vanishes for values  $\Delta_1^{XY} < -1$ . The numerical values of the remaining couplings are the same as in Fig. 7.

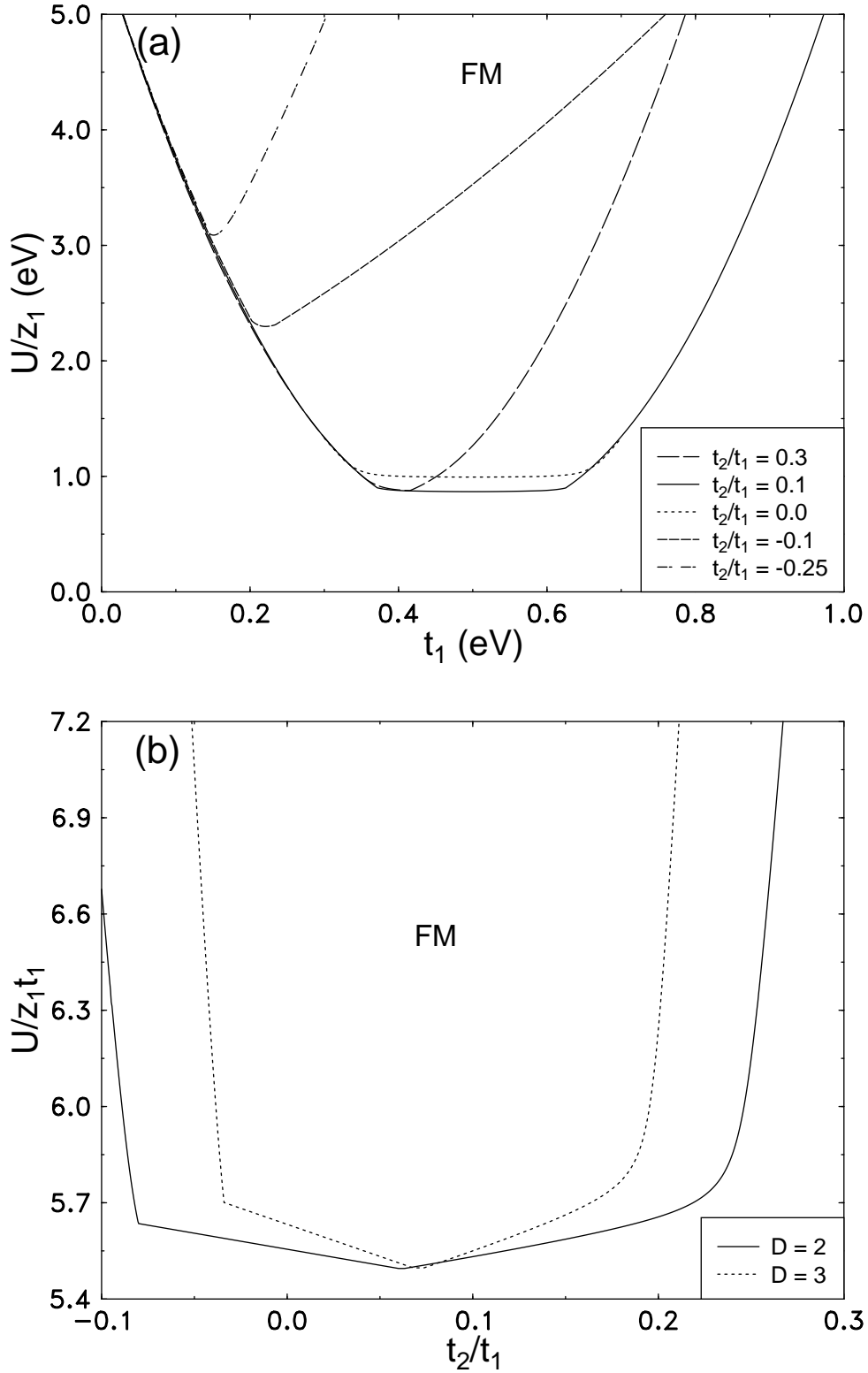


FIG. 9. Effects of next-to-nearest neighbor couplings on the stability of the fully saturated ferromagnetic state (FM) at half filling in the  $t_1$ - $U$  and  $t_2$ - $U$  planes, plot (a) and (b), respectively. Plot (a) shows the phase boundaries for various ratios of  $t_2/t_1$  choosing the numerical values of nearest neighbor interactions as in Fig. 7. Next-to-nearest neighbor interactions for the plot are as follows:  $X_2 = 0.08$  eV,  $V_2 = \frac{1}{8}V_1$ ,  $Y_2 = \frac{1}{5}Y_1$  and  $J_2 = \frac{1}{5}J_1$ . In plot (b) all the interaction constants are expressed in units of  $t_1$  instead of units of eV. Above each line the ground state is the fully polarized ferromagnetic state.

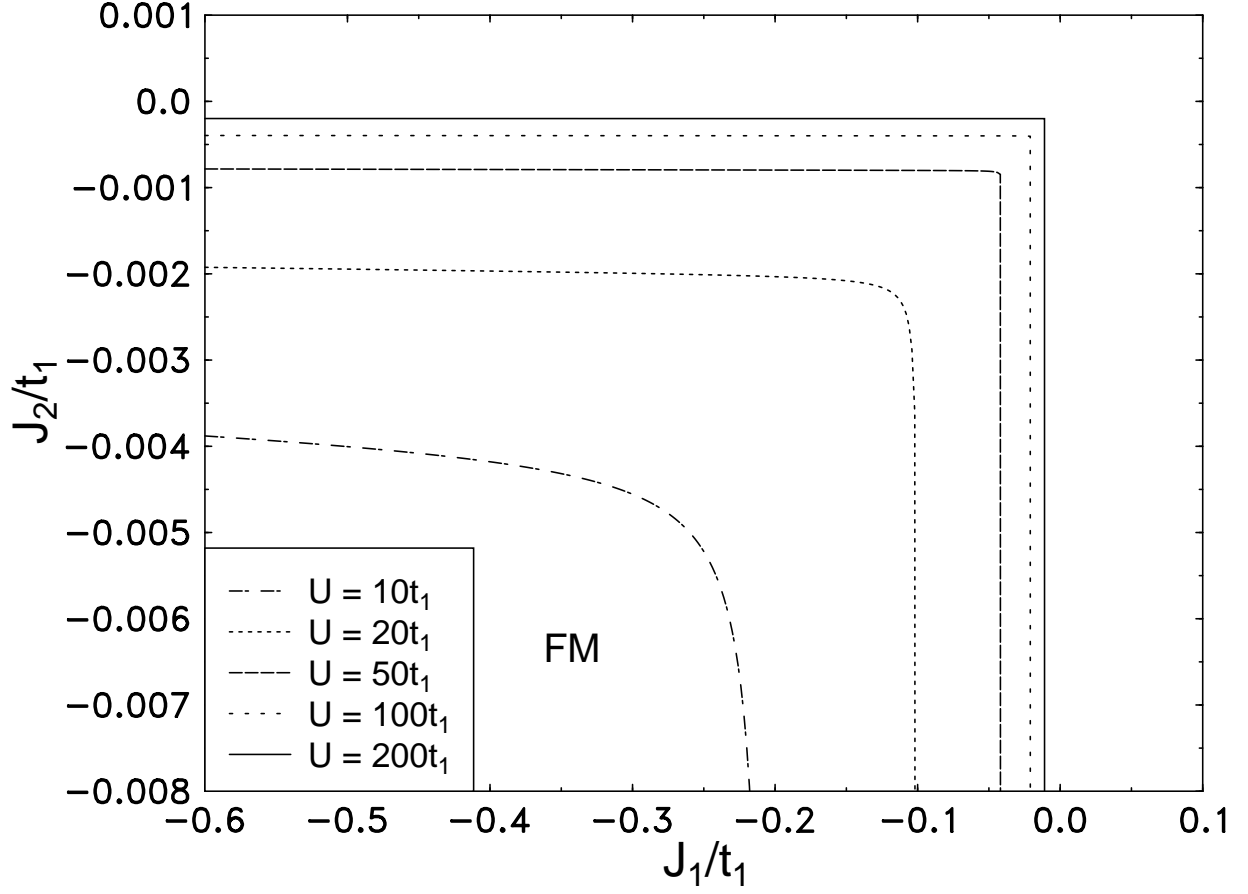


FIG. 10. Stability of the fully saturated ferromagnetic state (FM) in the presence of nearest ( $J_1$ ) and next-to-nearest ( $J_2$ ) neighbor exchange coupling at  $t_2 = -\frac{1}{10}t_1$ . All the other interactions are turned off, i.e.  $X_1 = X_2 = V_1 = V_2 = Y_1 = Y_2 = 0$ .